

Preparation and properties of $\text{Pb}(\text{Zr}, \text{Ti})\text{O}_3$ ferroelectric thin films and compositionally graded thin films on LaNiO_3/Si substrates

Li Jiankang · Yao Xi

Published online: 21 August 2007
© Springer Science + Business Media, LLC 2007

Abstract LaNiO_3 (LNO) thin films were prepared on Si (100) wafer by MOD method. $\text{Pb}(\text{Zr}, \text{Ti})\text{O}_3$ ferroelectric thin films and their compositionally graded thin films were prepared on LNO/Si (100) substrates by a modified sol–gel method. The composition depth profile of a graded film was determined by using a combination of Auger electron spectroscopy and Ar ion etching. The results confirmed that the processing method produces graded composition change. XRD analysis showed that the graded thin film possessed a composite structure of tetragonal and rhombohedral. The dielectric constant of the graded thin films was higher than that of each thin film unit, but the loss tangent was near to each other at 10 kHz. The temperature characteristics of the dielectric constant of the graded thin films at different frequencies showed three peaks and ferroelectric relaxor feature to some extent. Hysteresis loops showed that graded thin film had higher remanent polarization, smaller coercive field than each thin film unit. The pyroelectric coefficient of the graded thin films increased gradually with temperature, and was higher than that of each thin film unit.

Keywords Compositionally graded thin film · LaNiO_3 electrode · $\text{Pb}(\text{Zr}, \text{Ti})\text{O}_3$

1 Introduction

In recent years, ferroelectric thin films with a composition gradient have attracted much attention, because of their remarkable properties [1–3]. Graded ferroelectric devices (GFDs) are known to exhibit big dielectric constants and pyroelectric coefficients compared to conventional ferroelectric devices. However, most of these graded ferroelectric films were grown on Pt electrodes. It is well known that Pt electrodes often result in the formation of hillocks, which can electrically short the capacitors [4]. Furthermore, ferroelectric thin films on this kind of substrates have serious fatigue problems after long polarization switching cycles [5]. Recently, conductive perovskite oxides have been studied intensively as electrodes [6]. Among them, much attention has been drawn to the fabrication of metallic oxide LaNiO_3 (LNO) thin film, which is a pseudocubic perovskite with a lattice parameter of 0.384 nm. LNO thin film is a promising electrode material due to its desirable properties, such as low resistivity, excellent diffusion barrier properties, and good thermal stability [7–9]. Moreover, since LNO has the same crystal structure and similar lattice parameter to most of the perovskite-type ferroelectric materials including $\text{Pb}(\text{Zr}_x, \text{Ti}_{1-x})\text{O}_3$ (PZT) and $(\text{Ba}_x, \text{Sr}_{1-x})\text{TiO}_3$ (BST), it is highly expected that well-oriented ferroelectric films can be grown on the top of the LNO electrode.

In this paper, highly oriented conductive LaNiO_3 thin films were deposited on Si (100) substrates by a modified metalorganic decomposition technique and rapid thermal annealing method. Lead zirconate titanate (PZT) and their composition gradient thin films were prepared by a modified sol–gel technique on LNO/Si (100) substrates. The structural, dielectric, ferroelectric and pyroelectric properties of these thin films are reported.

L. Jiankang (✉)
Department of Applied Physics,
University of Science and Technology of Suzhou,
Suzhou 215011, China
e-mail: Ljk@mail.usts.edu.cn

Y. Xi
Electronic Material Research Laboratory,
Xi'an Jiaotong University,
Xi'an 710049, China

2 Experimental

LNO thin films were prepared by a modified metalorganic decomposition (MOD) on Si (100) substrates. Lanthanum nitrate [$\text{La}(\text{NO}_3)_3 \cdot 2.5\text{H}_2\text{O}$] and nickel acetate [$\text{Ni}(\text{CH}_3\text{COO})_2 \cdot 4\text{H}_2\text{O}$] were used as the starting materials, acetic acid and water were used as the solvents. Nickel acetate was dissolved in acetic acid and an equimolar amount of lanthanum nitrate was dissolved in distilled water at room temperature, respectively. Then the two solutions were mixed together with constant stirring. The concentration of the precursor solution was adjusted to 0.3 M by some acetic acid adding or distilling with water. The LNO precursor solution was passed through a 0.22 micron in-line syringe filter directly and spin-coated onto Si (100) substrates at 3,000 rpm for 30 s. After each coating, the film was fired at 160 °C for 300 s, then pyrolyzed at 400 °C for 360 s, and finally annealed at higher temperatures for 240 s. The process was repeated for four times to obtain thicker LNO films. The whole thermal treatment was completed in a RTA furnace. The thickness of the LNO electrodes was about 213 nm, and the room temperature resistivity was measured to be about $7.6 \times 10^{-4} \Omega\text{cm}$.

For fabricating PZT graded thin films, two PZT precursor solutions with varied Zr/Ti molar ratios were synthesized using a modified sol–gel process, in which, the two solid precursors of PZT were prepared first, and then the precursors were dissolved in 2-methoxyethanol (2-MOE) to form the sols for the spin-coating deposition [10]. The two compositions of the solutions are $\text{Pb}(\text{Zr}_{0.20}\text{Ti}_{0.80})\text{O}_3$ [PZT (20/80)] and $\text{Pb}(\text{Zr}_{0.80}\text{Ti}_{0.20})\text{O}_3$ [PZT (80/20)]. The precursor solutions were spin coated on LNO buffered Si (100) substrates in sequence: first PZT (20/80) solution, then PZT (80/20) solution. In this way, the PZT (80/20)/PZT (20/80)/LNO/Si graded thin film was formed. Each solution was spin coated three times. After each coating, the

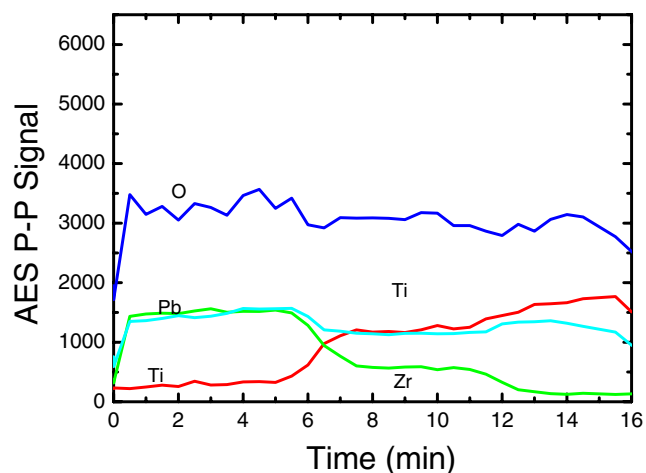


Fig. 1 Thickness distribution of compositions of the graded PZT thin film

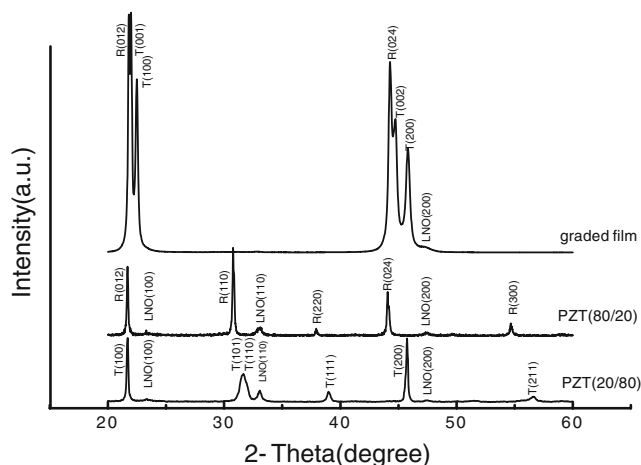


Fig. 2 XRD patterns of PZT (80/20), PZT (20/80) and the graded PZT thin films on LNO/Si (100) substrates

film was fired at 130 °C for 200 s, then at 380 °C for 240 s, and pyrolyzed at 460 °C for 240 s. Finally, the graded thin film was annealed at 650 °C for 240 s. The whole thermal treatment was completed in a RTA furnace. In order to compare the graded films with conventional thin films in structure and properties, the PZT (80/20) and PZT (20/80) thin films were prepared using the same heat treatment process.

The composition depth profile of the PZT graded thin film was determined by using a combination of Auger electron spectroscopy (AES, Model PHI-610/SAM) and Ar ion etching. The crystallographic orientation and the microstructure of the thin films were characterized by X-ray diffraction analysis (XRD, Model D8 advance) using nickel filtered $\text{Cu K}\alpha$ radiation. The dielectric constant–frequency (ϵ – f) properties were measured using a Hewlett-Packard (4284A) precision LCR meter at room temperature. Temperature characteristics of the dielectric constant of the graded thin film were measured using a Low Temperature Micro-probe (made by MMR Technologies INC) and Hewlett-Packard (4294A) precision LCR meter. Hysteresis loops were observed at 300 Hz using a Sawyer–Tower circuit (RT66A) at room temperature. Pyroelectric currents were measured using a Keithley 617 electrometer interfaced with a computer, at a constant heating rate of 2 °C/min in the steady state mode.

3 Results and discussion

Figure 1 shows the composition depth profile of the graded film determined by using a combination of Auger electron spectroscopy and Ar ion etching. It is obvious that the contents of Zr and Ti are changing with the depth in the upright direction of the thin film. The content of Ti increases with the etching depth, and Zr decreases with

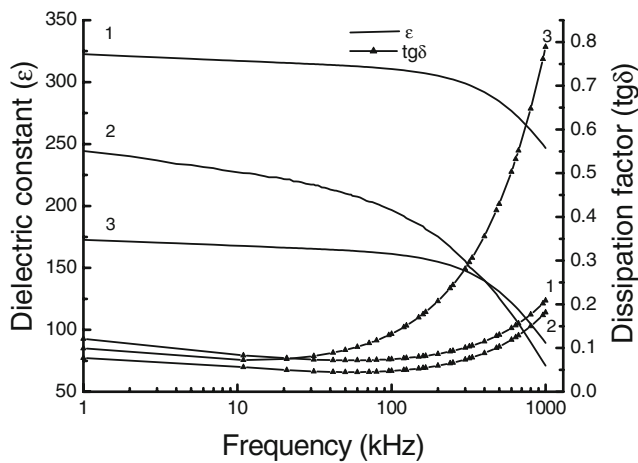


Fig. 3 The curves of ϵ - f and $\text{tg}\delta$ - f for PZT (80/20), PZT (20/80) and the graded PZT thin films on LNO/Si (100) substrates; 1 graded PZT thin film, 2 PZT (20/80) thin film, 3 PZT (80/20) thin film

the etching depth. The results confirm that the processing method produces a graded composition change, which is consistent with the expected results.

Figure 2 shows the XRD patterns for the graded thin film, PZT (80/20) and PZT (20/80) thin films annealed at 650 °C for 240 s in the RTA furnace. It can be seen that the structure of PZT (20/80) thin film is tetragonal and the structure of PZT (80/20) thin film is rhombohedral. In addition, the PZT (20/80) film and the graded thin film shows strong (100) preferred orientation, while the PZT (80/20) thin film shows random orientation. The difference is believed to be due to the composition at the film/substrate interface is because the structure of PZT (20/80) film is similar to that of the LNO thin film. They are both tetragonal perovskite phase. In addition, Fig. 2 shows that the graded thin film possesses diffraction peaks of PZT (80/20) and PZT (20/80) thin films, so the graded thin film is a composite structure of tetragonal and rhombohedral.

The dielectric properties were measured on films in a metal–insulator–metal configuration. Figure 3 shows the variation of the dielectric constants and dissipation factors

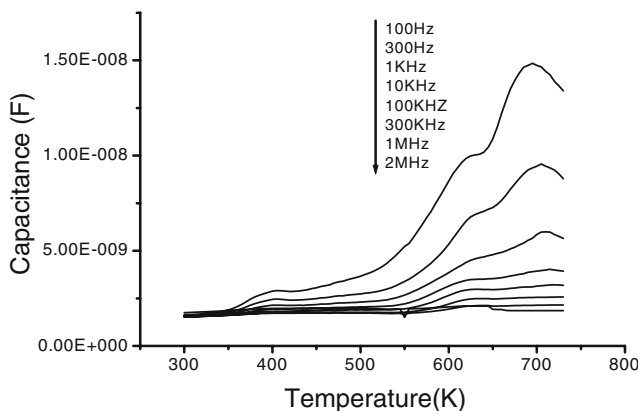


Fig. 4 Temperature dependent of the dielectric constant at different frequencies for the graded PZT thin film on LNO/Si (100) substrate

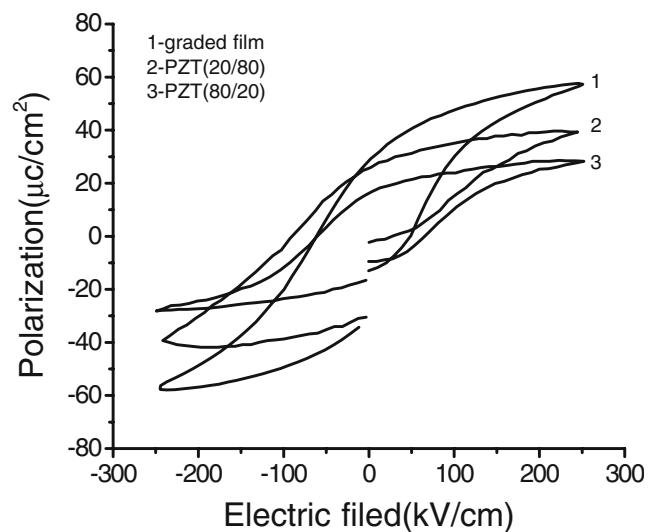


Fig. 5 The hysteresis loop for PZT (80/20), PZT (20/80) and the graded PZT thin films on LNO/Si (100) substrates

with the frequency in the range of 1–1,000 kHz for the graded films, PZT (80/20) and PZT (20/80) deposited on LNO/Si (100) substrates. It can be seen that the dielectric constant of the graded thin film is higher than that of PZT (80/20) and PZT (20/80) thin films, but the dissipation factors are close to each other at 10 kHz. The dielectric constant and dissipation factor of the graded thin film are 317 and 0.057 at 10 kHz, respectively.

Figure 4 shows temperature characteristics of the dielectric constant of the graded thin film at different frequencies. It can be seen that there are three distinct peaks in the curves of ϵ - T at every frequency. The peak temperatures are about 400, 625 and 700 K, respectively. According to the PbZrO_3 - PbTiO_3 solid solutions phase diagram, the three peaks are the $F_R(\text{LT})$ - $F_R(\text{HT})$ phase transition temperature, the rhombohedral phase Curie temperature and the tetragonal phase Curie temperature,

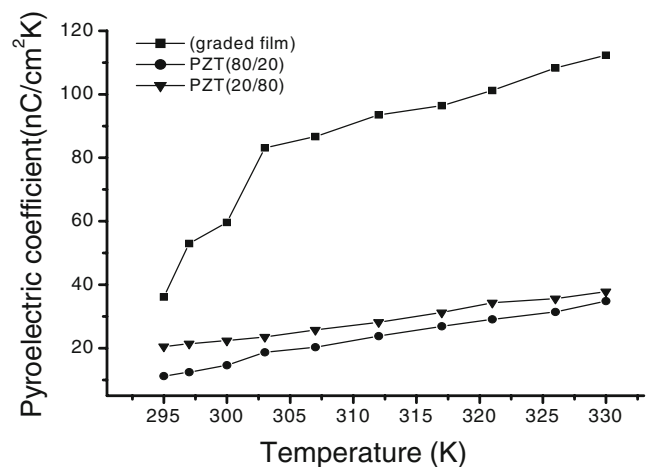


Fig. 6 The curves of p' - T for PZT (80/20), PZT (20/80) and the graded PZT thin films on LNO/Si (100) substrates

respectively. It illustrated that the graded thin film possessed a composite structure of tetragonal and rhombohedral phases. On the other hand, because of three peaks in the curves of $\epsilon-T$, the dielectric constant has a broad distribution over a wide temperature range, which gives the temperature coefficient of the dielectric constant a relatively small variation. It is advantageous for applications of the graded thin films, especially in uncooled pyroelectric IR Sensors.

In addition, Fig. 4 shows ferroelectric relaxor phenomena to some extent in the curves of $\epsilon-T$. Dielectric constant peaks shift to high temperature with increasing frequency. It was reported that this behavior is a consequence of a space charge field. In the graded thin films the space charge field is built up on the internal face between layer and layer by the redistribution of the defects and/or space charge. It will introduce some new applications of the graded thin films for ferroelectric relaxor feature.

Figure 5 shows the hysteresis loops of the graded film, PZT (80/20) and PZT (20/80) thin film on the LNO/Si (100) substrate. It is apparent that the remnant polarization (P_r) of the graded film is higher than that of PZT (80/20) and PZT (20/80) thin films. It may be due to the composite structure of the graded film. The remnant polarizations (P_r), average of the positive and negative values, were estimated to be approximately 29.96, 22.24 and 21.19 $\mu\text{C}/\text{cm}^2$ for the graded film, PZT (80/20) and PZT (20/80) thin film, respectively. The approximate coercive field (E_c) of 54.12 kV/cm for the graded film, 59.8 kV/cm for PZT (80/20) thin film, and 64.62 kV/cm for PZT (20/80) thin film were obtained.

Figure 6 shows the temperature characteristics of the static pyroelectric coefficients for PZT (80/20), PZT (20/80) and the graded PZT thin films. None of the films were polarized before testing. It can be seen that the pyroelectric coefficient of the films showed a gradual increase with temperature. The pyroelectric coefficient of the graded film is higher than that of PZT (80/20) and PZT (20/80) thin films. It may also be due to the composite structure of the graded film. The pyroelectric coefficient of, PZT (80/20), PZT (20/80) and the graded thin film are 12.4, 21.4, and 53.1 $\text{nC}/\text{cm}^2 \text{K}$ at room temperature, respectively.

4 Conclusions

LaNiO₃ (LNO) thin films were prepared on Si (100) wafer by MOD method. PZT (80/20), PZT (20/80) and their compositionally graded thin films were prepared on LNO/Si (100) substrates. The composition depth profile confirmed that the processing method produces graded composition change. XRD analysis showed that the graded thin film possessed strong (100) preferred orientation and a composite structure of tetragonal and rhombohedral. The dielectric constant and dissipation factor of the graded thin film are 317 and 0.057 at 10 kHz, respectively. The temperature characteristics of the dielectric constant of the graded thin films at different frequency showed a F–F phase transition temperature and two Curie temperatures. The remnant polarization (P_r) were estimated to be approximately 29.96, 22.24 and 21.19 $\mu\text{C}/\text{cm}^2$ for the graded film, PZT (80/20) and PZT (20/80) thin film, respectively. The pyroelectric coefficient of the graded film, PZT (80/20) and PZT (20/80) thin film are 12.4, 21.4, and 53.1 $\text{nC}/\text{cm}^2 \text{K}$ at room temperature, respectively.

Acknowledgements This work was supported by the Jiangsu Provincial Natural Science Foundation (No. BK2005039) and the Jiangsu University Natural Science Research Project (No. 05KJB430127).

References

1. X.G. Tang, H.L.W. Chan, A.L. Ding, *Solid State Commun.* **127**, 625 (2003)
2. S. Callard, A. Gagnaire, J. Joseph, *Thin Solid Films* **313**, 384 (1998)
3. B. Vilquin, G. Poullain, R. Bouregba, et al., *Thin Solid Films* **436**, 157 (2003)
4. Z.T. Song, C.L. Lin, *Appl. Surf. Sci.* **158**, 21 (2000)
5. S. Thakoor, *J. Appl. Phys.* **75**, 409 (1994)
6. C. Pollak, K. Reichmann, H. Hutter, *Surf. Coat. Technol.* **150**, 119 (2002)
7. X.J. Meng, J.L. Sun, J. Yu, et al., *Appl. Surf. Sci.* **171**, 68 (2001)
8. S. Miyake, S. Fujihara, T. Kimura, *J. Eur. Ceram. Soc.* **21**, 1525 (2001)
9. K.P. Rajeev, G.V. Shivashankar, A.K. Raychauduri, *Solid State Commun.* **79**, 591 (1991)
10. W.G. Liu, J.S. Ko, W.G. Zhu, *Thin Solid Films* **371**, 254 (2000)